Strength and fracture of TWIP steel dissimilar weld joints

P. Russo Spena
Faculty of Science and Technology, Free University of Bozen-Bolzano, Bolzano (Italy)
pasquale.russospena@unibz.it

P. Matteis, A. Sanchez, G. Scavino
Department of Applied Science and Technology, Politecnico di Torino, Torino (Italy)

ABSTRACT. Car-bodies are more and more frequently made with advanced high-strength steels, both to reduce vehicles weight and to improve passenger safety. Car-body parts are usually hot or cold formed by using several different steel sheet grades, and are then assembled by welding. In the last years, new high-manganese steels, called TWIP, have been proposed for fabricating car body parts due to their excellent combination of strength and toughness. These steels have an austenitic structure which is strengthened by carbon and by the possibility to deform via mechanical twinning (TWIP: TWinning Induced Plasticity). However, a widespread usage of TWIP steels for car body parts is conditional on the employment of appropriate welding methods, especially if dissimilar welding must be performed with other automotive sheet steel grades. The discontinuous resistance spot welding (RSW) is currently prevalent in assembling car body parts; however, the mechanical properties of RSW joints are often unsatisfactory, and always much lower than those of base metals, due to the relevant notch effects. Therefore, improvements might be obtained by welding advanced automotive steels with continuous techniques. For these reasons, dissimilar continuous butt welding between TWIP steel sheets and two frequently employed high strength automotive steel sheet grades is examined here. The metal active gas (MAG) welding technique was employed to join TWIP steel with either a martensitic boron-alloyed hot-forming steel or a Dual Phase cold-forming one. Thereafter, the weldments were characterized by metallography and microhardness tests. A series of tensile specimens, cut perpendicular to the welding line, were also tested and then subjected to fractographic examinations.

SOMMARIO. Le scocche delle autovetture sono sempre più spesso prodotte con acciai innovativi ad alta resistenza, sia per ridurre il peso dei veicoli che per migliorare la sicurezza dei passeggeri. Le parti della scocca sono generalmente ottenute mediante processi di deformazione plastica a caldo o a freddo, utilizzando diversi tipi di acciai sotto forma di lamiera, che vengono poi assemblati mediante saldatura. Negli ultimi anni, nuovi acciai ad alto tenore di manganese, denominati TWIP, sono stati proposti per la fabbricazione di scocche di autoveicoli, per la loro eccellente combinazione di resistenza meccanica e tenacità. Questi acciai hanno una struttura austenitica che viene rafforzata sia dal carbonio, presente come elemento di lega, che dalla possibilità di tale struttura di deformarsi plasticamente attraverso geminazione meccanica (TWIP, TWinning Induced Plasticity). Tuttavia, l'utilizzo dell'acciaio TWIP nelle scocche degli autoveicoli è subordinata all'impiego di adeguati metodi di saldatura, soprattutto se esso deve essere saldato con altri tipi di acciai ad alta resistenza. La saldatura per resistenza a punti (RSW) è attualmente il metodo di giunzione più diffuso nell'assemblaggio dei componenti della scocca degli autoveicoli; tuttavia, le proprietà meccaniche dei giunti così saldati sono spesso insoddisfacenti, e sempre molto inferiori a quelle dei metalli base, a causa dei rilevanti effetti di intaglio. Pertanto, la qualità dei giunti saldati di acciai alto resistenziali potrebbe essere migliorata utilizzando tecniche di saldatura continue. Per queste ragioni qui sono esaminate le proprietà dei giunti di saldatura testa a testa tra

lamiere di acciaio TWIP e di due altri acciai ad alta resistenza utilizzati in ambito automobilistico. La saldatura MAG è stata impiegata per la giunzione dell'acciaio TWIP sia con un acciaio legato al boro a matrice martensitica che con un acciaio Dual Phase. Successivamente, i giunti saldati sono stati caratterizzati mediante metallografia e test di microdurezza. Una serie di provini di trazione, tagliati perpendicolarmente alla linea di saldatura, sono stati anche testati meccanicamente e poi sottoposti ad analisi frattografica.

KEYWORDS. TWIP steel sheet; Welding joint; Microstructure; Mechanical properties; Fracture.

INTRODUCTION

Along with the intensifying of environmental pollution problems, energy saving has become the most important issue for automotive manufacturers. Among the many measures in reducing fuel consumption and CO_2 emission, reducing the weight is one of the most effective: a study have demonstrated that 10% of weight reduction leads to 3-7% less of fuel consumption [1]. Another important goal for manufacturers is to increase passenger safety, thus car-body structures should have higher and higher energy absorption to improve frontal and side impact and roof crash performances. To address both these tendencies, the amount of high strength steel (HSS) used in automotive industry for fabricating sheet components is gradually increasing and new advanced high strength steels (AHSS) are under development. Research activity is focused on an increase of the mechanical strengths along with the preservation, or improvement, of ductility. The increase of strength enables car manufacturers to reduce the overall weight of vehicles, while improved ductility allows to increase energy absorption during a crash event as well as to produce components with more complex geometry [2-5].

To date, the most important HSS/AHSS used to yield automotive sheet components are DP and boron-alloyed hot-forming (Mn-B) steels. DP are low carbon-manganese steels having a ferritic and martensitic microstructure; the amount of martensite usually range from 5% to 20%. The tensile strength of DP steels increases with the martensite content ranging from 500 to 1200 MPa. DP steels are also characterized by a low ratio between the yield stress and the ultimate tensile strength, by a high work hardening exponent and by a good cold formability, thus they are widely used to cold form components that require high strength and good crashworthiness (e.g.: bumpers, pillar reinforcements). Mn-B steels are hardenable steels alloyed with boron and manganese and coated with an aluminum-silicon layer. Unlike DP steel grades, Mn-B ones are hot formed: the blank is heated to about 900 °C, stamped and then rapidly cooled (quenched) to room temperature in the water-cooled forming mold. In this way, tensile strength even superior to 1500 MPa and adequate ductility can be achieved. The aluminum-silicon coating is especially designed to protect the steel from both high-temperature oxidation, during the forming process, and in service corrosion. Mn-B steel grades are widely used to fabricate components that require high strength (e.g., anti-intrusion bars).

In the last years, new high-manganese steels, called TWIP (TWinning Induced Plasticity), have been proposed for fabricating car-body parts due to their excellent combination of strength and toughness. TWIP steels contain a high amount of manganese (15-25 wt.%) and have a fully austenitic microstructure. These steels exhibit exceptional combination of strength and ductility due to predominant strengthening mechanism by twinning: the formation of mechanical twins during deformation generates high strain hardening, preventing necking, and thus maintaining a very high strain capacity. Fracture elongation superior to 50% and tensile strenght more than 1000 MPa are usually obtained [6-13].

Automotive sheet components in TWIP steels are still under development and, unless rare cases, only prototypal components have been fabricated at the moment. However, according to several material suppliers, about 15% of the body structure of a vehicle will be made out of TWIP parts in the next 5-10 years [14].

As many of the automotive components must be assembled by welding or welded prior to forming operations (taylor welded blanks), the evaluation of the mechanical and microstructural response of dissimilar joints of AHSS is of primary importance for their full exploitation in the automotive industry.

The mechanical properties and formability of dissimilar welded steel sheet depend considerably on the extensive heating, melting, and solidification stages during welding process. Therefore, welding input parameters play a very significant role in integrity and quality of a weld joint, and hence in fabrication of welded automotive sheet components. Regardless of the type of heating source (laser, electric arc), heating power, welding velocity, distance between the steel surface and the torch, focal position are some of process parameters that have to be accurately controlled to obtain an optimal welded

seam [15]. Many studies have already studied the effect of many welding parameters on several steel grades (carbon steels, stainless steels, low alloy steels, etc.) [12, 16-18] and several relationships between the process parameters (e.g., beam power, welding speed and beam incidence angle) and the weld bead parameters (e.g., penetration, bead width and area of penetration) have been developed. However, the evaluation of the mechanical and microstructural response of dissimilar joints of TWIP, DP, and Mn-B steel sheets after arc and laser welding is not well studied; only a few researches have been carried out on dissimilar welding of AHSS sheets [19-21].
For this reason, this work aims at investigating the response of dissimilar weld seams of TWIP, DP, and Mn-B steel sheets after MAG welding. The joints have been studied from a mechanical and microstructural standpoint. More specifically, the influence of welding process parameters on the mechanical strength, hardness, and microstructure has been analyzed in detail. Optical microscopy have been used to detect the metallurgical constituents occurring in the microstructures and to differentiate the fusion zone, the heat-affected zone, and the base material. Thereafter, a series of tensile specimens, cut perpendicular to the welding line, have been mechanically tested and subjected to fractographic examinations.

EXPERIMENTAL

The TWIP steel is a Fe–22Mn–0.5C alloy produced on industrial scale by continuous casting, hot and cold rolling, and continuous annealing, as a 1.6 mm thick sheet. The DP steel is a commercial sheet of DP600 with a thickness of 1.8 mm. The Mn-B steel is a commercial sheet with a thickness of 1.5 mm. The steels nominal chemical compositions is listed in Tab. 1.

Steel	C	Si	Mn	Cr	Mo	Al	Ti	V	B
TWIP	0.51	0.16	22.4	0.14	0.70	-	-	0.22	-
DP	0.09	0.21	1.65	0.43	-	0.030	0.003	-	-
Mn-B	0.25	0.23	1.30	0.13	-	0.036	0.039	-	0.0047
307L	0.07	0.65	6.5	18.5	-	-	-	-	-

Table 1: Chemical composition (%wt.) of the examined TWIP, DP, and Mn-B steels, and of the 307L welding filler. P+S<0.03% in all cases.

Dissimilar butt-joints of the TWIP/DP and TWIP/Mn-B steels were produced by welding using the MAG technique (Fig. 1). An AISI 307L steel wire was used as a consumable electrode during the welding operations, its nominal chemical composition is also listed in Tab. 1. The welding penetration was inhomogeneous along the welding line, ranging from 0.5 mm to the full sheet thickness.
Optical microscopy was performed on metallographic cross-section of the welded joints, in positions exhibiting full weld penetration, which were mechanically ground and polished and then etched using nital (3% HNO_3 in ethanol).
The same samples were also used for Vickers microhardness tests (HV0.1). The measurements were carried out perpendicularly to the welding line in order to evaluate the mechanical inhomogeneity arising from the microstructures occurring after the welding process (fusion zone, heat-affected zone, and base material). Line profiles were taken with a step size of 0.15 - 0.3 mm.
Flat tensile specimens (80 mm gage length), cut in the direction perpendicular to the weld seam, were tested at room temperature by a servohydraulic testing system under 0.2 mm/s actuator displacement control. The fractured surfaces were then subjected to fractographic examinations by optical and scanning electron microscopy. The specimens exhibiting an incomplete weld penetration on their fracture surface were not used to calculate the tensile properties; in the other cases the fracture always occurred in a HAZ, and the fracture stress was calculated by considering the original cross section of the specimen on the side in which the fracture occurred, in order to consider the slight difference in thickness between the two halves of each specimen. Standard tensile tests were also performed on the as-fabricated steels for comparison.

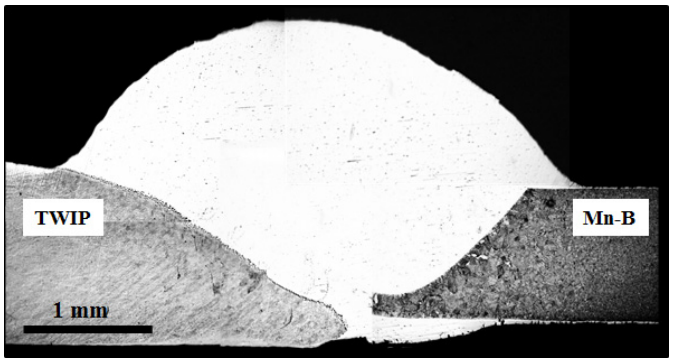

Figure 1: Overview of a butt welded joints between TWIP and Mn-B steels.

RESULTS AND DISCUSSION

Microstructure

The microstructure of the TWIP sheet is fully austenitic with a rather homogeneous grain size, around 3 μm on average (Fig. 2-a). The occurrence of other phases or precipitates was not detected, neither by the optical metallographic analysis nor by the X-ray diffraction analysis, which heads to the conclusion that the carbon and the other alloy elements are completely solubilized in the austenitic matrix. DP shows the typical dual-phase microstructure (Fig. 2-b): the light phase is ferrite, while the dark one is martensite. The martensite phase is homogeneously distributed in the ferrite matrix with about a 15% volume fraction. The average grain size of ferrite is around 10 μm. The Mn-B steel exhibits a microstructure of martensite homogenously distributed (Fig. 2-c).

No significant micro-hardness difference was detected on the sheet cross section of the base materials; thus it can be concluded that the previous production and sampling procedures have not introduced sensible mechanical inhomogeneity in the sheet thickness.

The fusion zone was not affected by metallographic etching, because the filler metal was a stainless steel. Overall, the average grain size has increased in the vicinity of the fusion zone, up to 40-50 μm in the TWIP steel (Fig. 3-a), 20-30 μm in the DP steel, and 100 μm in the Mn-B steel (Fig. 3-b).

In both the dissimilar weldements, the TWIP steel does not exhibit any significant changes in the microstructure beyond 4 mm from the fusion zone. Fig. 3-a indicates that the austenitic grains tend to be dissolved as the steel melted. These findings are consistent with previous studies of the HAZ of TWIP joints [17, 22].

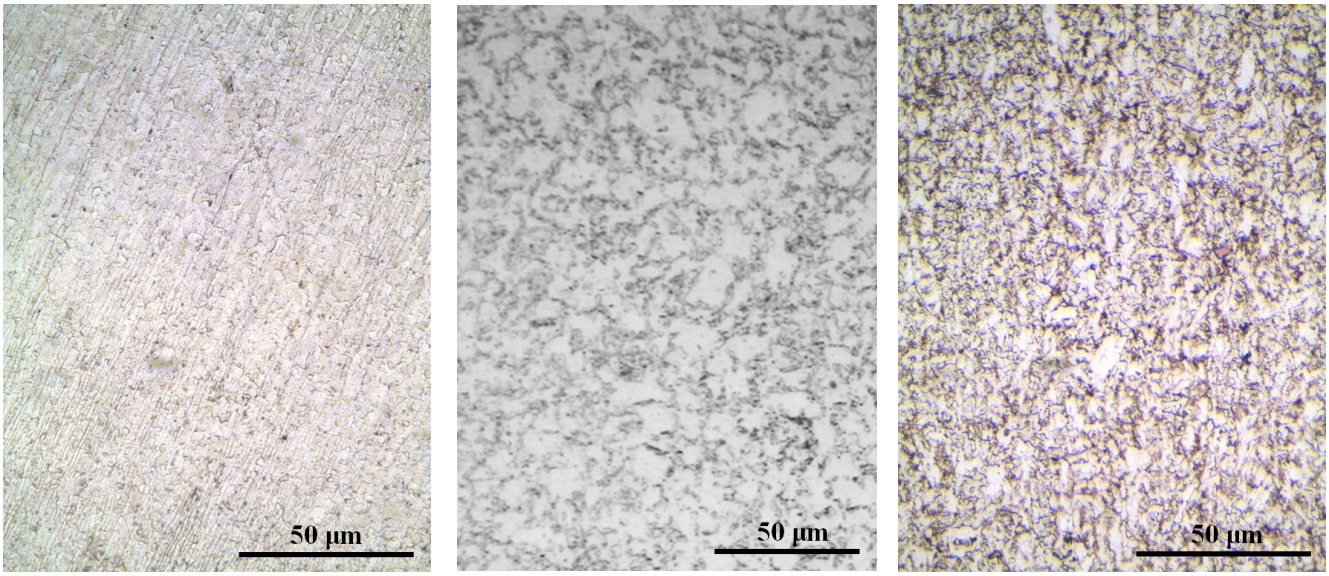

(a) (b) (c)

Figure 2: Microstructures of the TWIP (a), DP (b), and Mn-B (c) steels in the as-fabricated conditions.

The HAZ of the DP steel exhibits two different regions; white regions refers to ferrite, while darker areas are related to martensitic microstructures (in this last case the presence of bainite cannot be excluded). The HAZ in contact directly with the fusion zone, where the material was austenitized, consists of martensite; moving away from the fusion zone the HAZ is mainly formed by ferrite and tempered martensite.

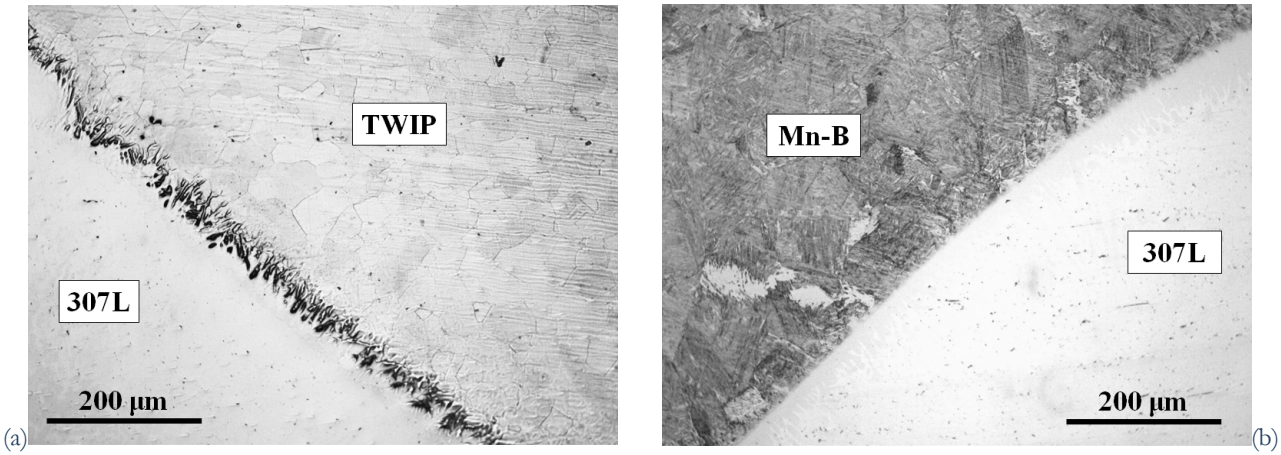

(a) (b)

Figure 3: Metallographic examination of the TWIP/DP (a) and TWIP/MnB (b) weld seams. Fusion zone (not etched) and HAZ.

Microhardness

The microhardness line profiles are shown in Fig. 4. The fusion zones exhibit, in all cases, hardness values comprised between 210 and 250 HV0.1, with a large scatter. The Vickers hardness of TWIP steel is about 270 HV0.1. Regardless of the welding counterpart, the HAZ of the TWIP steel exhibits a hardness generally lower than 250 HV0.1, in particular it decreases down to 200 HV0.1 close to the fusion zone due to the softening and coarsening of the austenitic grains during welding process. Also the extent of HAZ of TWIP steel, evaluated by hardness profile, does not change significantly in all the weldments, ranging from 2 to 3 mm. The hardness of the DP steel, far away from the weld seam, was about 225 HV0.1. In the HAZ, close to the fusion zone, the DP hardness exhibits a much higher maximum value of 360 HV0.1, which is attributed to a full austenitization followed by the martensitic transformation on cooling. In the HAZ farther away from the fusion zone, the DP hardness exhibits a minimum value of 200 HV0.1, which is attributed to the subcritical tempering of the original microstructure. The hardness of the Mn-B in as-fabricated condition is 485 HV0.1. This hardness is greater than the one reached in the DP base material. The hardness values found in the HAZ of the Mn-B steel, range from 254 to 457 HV0.1, which is explained as follows: the Mn-B is fully martensite close to the fusion zone where the maximum hardness values have been reached, while at the end of the HAZ the hardness is lower than 200 H0.1 due to the tempering effect occurred in these zones during welding process. It can be pointed out that that the HAZ zone in the Mn-B side is by far larger than the DP ones in the other samples, while the extent of the HAZ of the TWIP side does not significantly change in both types of samples due to the similar welding conditions used in the welding tests.

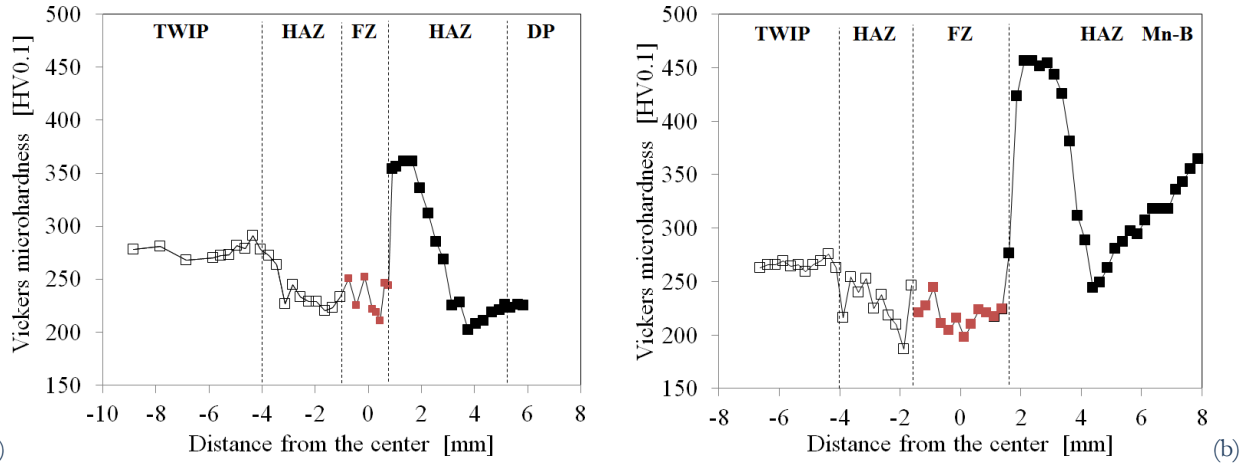

(a) (b)

Figure 4: Vickers microhardness profile across the TWIP/DP (a) and TWIP/Mn-B (b) weldments.

Tensile tests

The results of the tests excluding the specimens exhibiting incomplete weld penetration are shown in Tab. 2. TWIP steel exhibits a yield stress similar to DP one, even though the tensile strength and the elongation at fracture are much higher. Mn-B steel shows the highest yield stress and tensile strength, but the lowest elongation at fracture. Regardless the nature of the steels, weldments exhibits a yield stress and an elongation at fracture quite similar, while the most significant differences are obtained in tensile strength values. This clearly indicates that the yield bevahior of welded joints was mainly affected by TWIP steel (which has the lowest yield stress), while tensile strength behavior results from a combination of both materials. In particular, it can be pointed out that the TWIP/Mn-B weldments exhibits, in respect with TWIP/DP one, the higher tensile strength.
Overall, fractures occurred either in the HAZ or in the fusion zone, which is consistent with the fact tensile properties and plastic deformation of the welded joints are smaller than respective base materials. Another important point to consider is that martensite was found in some regions of HAZ zone in DP and Mn-B materials.

Steel	$Rp_{0.2}$ [MPa]	Rm [MPa]	e_f [%]	Fracture region
TWIP	460	1005	45	-
DP	470	690	19	-
Mn-B	1050	1440	5	-
TWIP/DP	-	700*	18*	FZ, DP HAZ
TWIP/Mn-B	-	880*	16*	FZ, TWIP and Mn-B HAZs

Table 2: Tensile properties of the base material and relative welded joints of TWIP, DP, and Mn-B steels. *The values are calculated considering as specimen area the mean of the areas of as-fabricated sheet steels.

Fractography

The fracture surfaces of the tensile specimens were investigated to analyze the fracture mechanism of steels in as-fabricated and welded conditions. The steels in as-fabricated condition mainly exhibit ductile fractures with the occurrence of dimples, Fig. 5. In particular, the fracture surfaces of TWIP steels show some zones fractures by shearing, thus forming some flat areas among dimples ones, Fig. 5-a. This phenomenon is may be promoted by the occurrence of twinning mechanisms during plastic deformation of this steel. The fracture surfaces of Mn-B, overall, also appears with notably plastic deformation, Fig. 5-b.

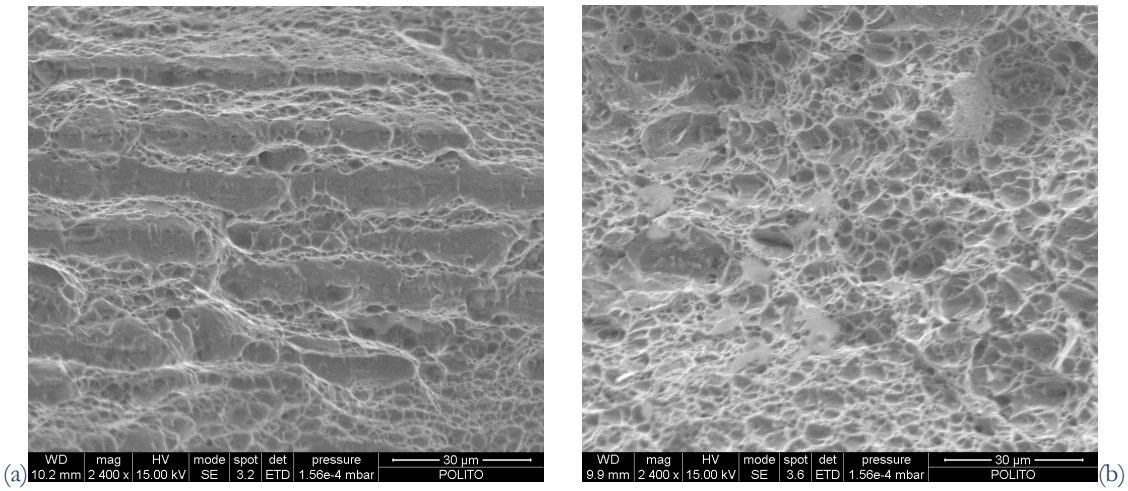

Figure 5: Fracture surfaces of TWIP and Mn-B tensile specimens.

The fracture of tensile specimens of TWIP/Mn-B occurs in the HAZ of either steels. Sometime the fractures is located in the interface between HAZ and fusion zone. In the case of a fracture in Mn-B side, fracture surfaces again exhibit a cone-

cope fracture, Fig. 6-a, with the occurrence of dimples area, even though the extent of the last ligaments among dimples is much less pronounced in respect to the base material, Fig. 6-b. Cleavage facets are nearly absent.

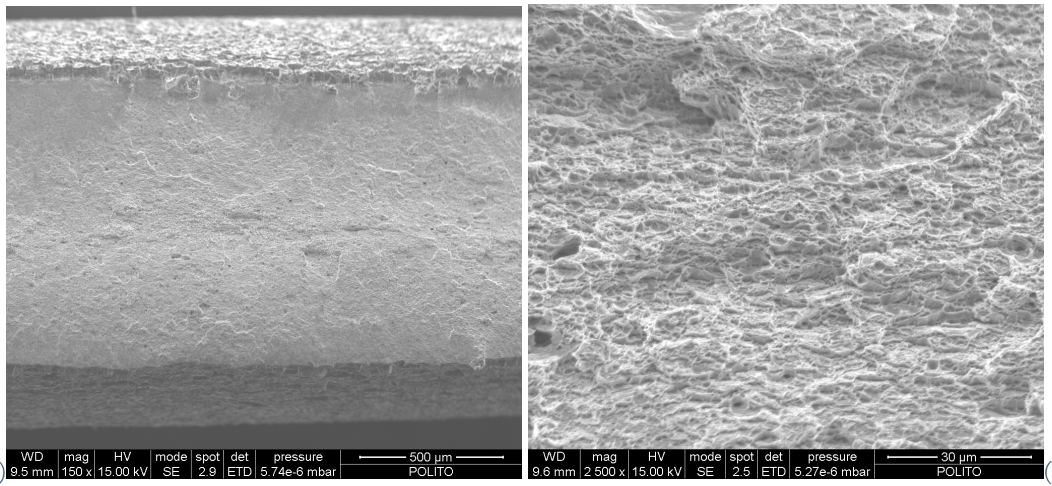

(a) (b)

Figure 6: Fracture surfaces of TWIP/Mn-B welded joint. Fracture in the HAZ of Mn-B steel. Macroscopic (a) and microscopic (b) views.

In the case of a fracture in TWIP side, fracture surfaces again exhibit a fully ductile fracture surface. Thus, a similar fracture surface to the TWIP steel in as-fabricated condition is obtained. The grain coarsening of austenitic grains in HAZ do not seem to affect the size of dimples and shear lips, even though shear zones are less numerous that in the case of TWIP in as-fabricated conditions.

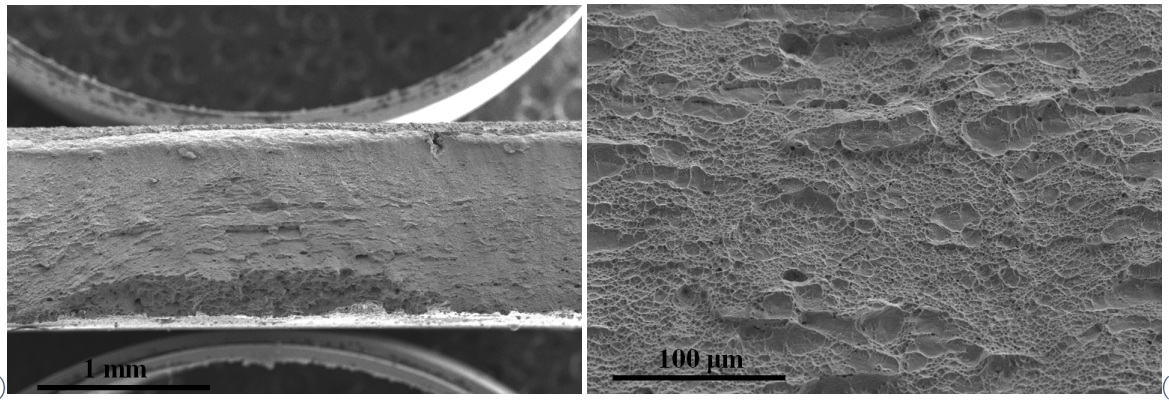

(a) (b)

Figure 7: Fracture surfaces of TWIP/Mn-B welded joint arising from incomplete weld penetration. Fracture in the interface between fusion zone and HAZ of TWIP steels. Macroscopic (a) and microscopic (b) views.

It must be noted that specimens with an incomplete weld penetration exhibit tensile properties notably less than full welded joints, in some cases a reduction of 30-40% of tensile strength has been obtained. In these cases, the tensile specimens exhibit a brittle mechanical behaviour, with fracture surfaces showing primarily the occurrence of large cleavage facets. In some cases, e.g. when the fracture occurs in the HAZ of the Mn-B steels, dimples are completely absent, Fig. 8. The fracture of tensile specimens of TWIP/DP only occurs in the HAZ of DP steel. Sometime the fractures is located in the fusion zone, but never in the TWIP side. The tensile specimens do not exhibit a macroscopic plastic deformation, Fig. 9-a. Fracture surfaces exhibits a mixed morphology, dimples areas occur along with cleavage facets.

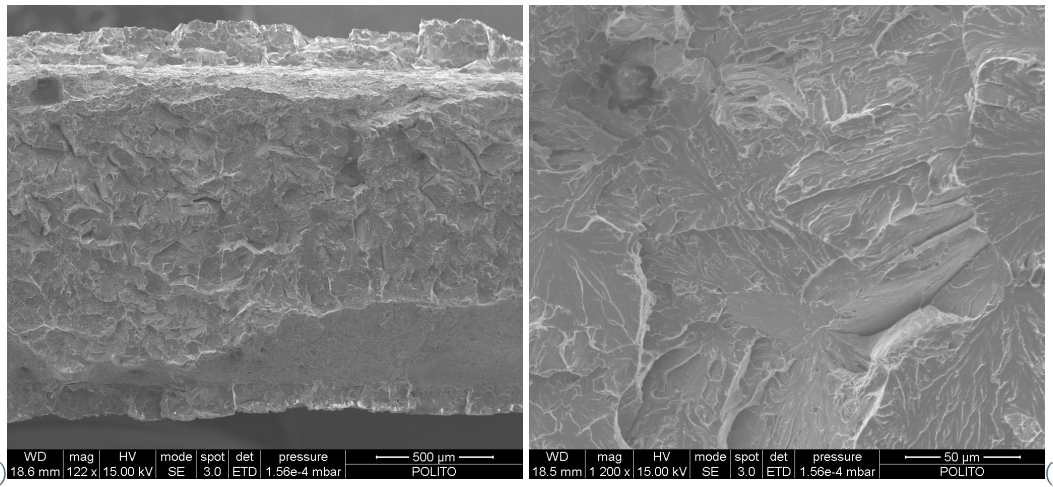

(a) (b)

Figure 8: Fracture surfaces of TWIP/Mn-B welded joint with notch. Fracture in the interface between fusion zone and HAZ of Mn-B steels. Macroscopic (a) and microscopic (b) views.

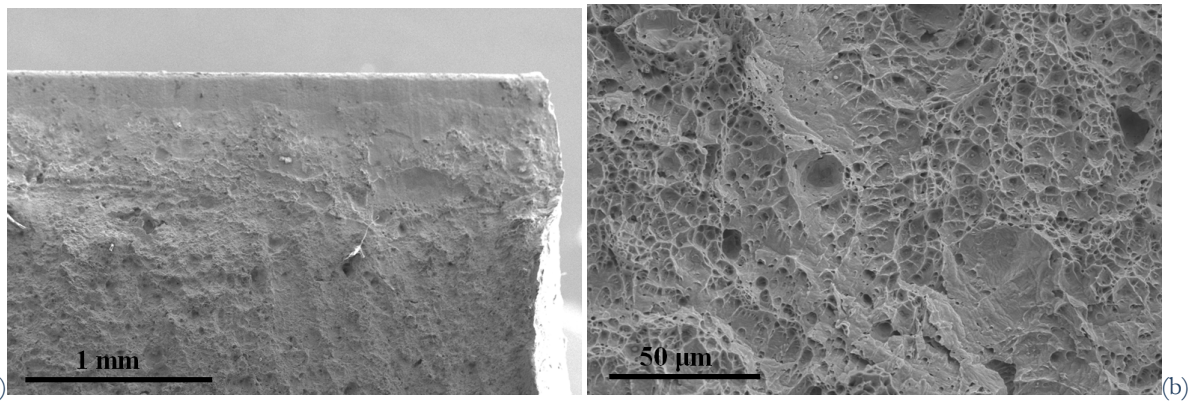

(a) (b)

Figure 9: Fracture surfaces of TWIP/DP welded joint. Fracture in the HAZ of DP steel. Macroscopic (a) and microscopic (b) views.

CONCLUSIONS

Dissimilar joints of TWIP with DP and a martensitic boron-alloyed hot-forming steels were produced by MAG welding and characterized with respect to the microstructure, mechanical properties, and tensile fracture surfaces.

Under the applied welding conditions, the HAZ of TWIP steel consists in enlarged austenitic grain sizes, of an order of magnitude in respect to the initial grain size, while phase transformations occur in DP and Mn-B steels. Fully martensitic microstructures occurs in the HAZ of the DP and Mn-B steels close to the fusion zone. The volume fractions of metallurgical phases in DP steel (martensite and ferrite), as well as the grain morphology have been significantly altered within this region. Newly formed martensite was also detected in the HAZ of the Mn-B steel.

A larger HAZ was identified in Mn-B steel in respect with the HAZ occurring in welded joints of TWIP and DP steels. Furthermore, the difference between the maximum and minimum hardness in Mn-B is higher that the one in the DP part; however, the hardness of the Mn-B steel in base material is much higher that the DP one. This is due to the lower content of carbon in DP steel and to the tempering of the fully martensitic microstructure of the Mn-B steel during the operation, that, instead, affects only the martensite (about 15% vol.) present in the DP steel and not the ferrite. Microstructure of TWIP does not present notably differences in two different types of welded joints (similar HAZ extent and hardness profile).

The fracture of the tensile specimens can occur in different position of the weld seams. In the TWIP/DP weldments, fractures occur either in the fusion zone or in the HAZ of DP steels. In the TWIP/Mn-B steels, they occur either in the

HAZ of the TWIP or Mn-B steels. In some cases, when the lowest values of tensile properties were obtained, the butt welded joints fractured in the interface between the fusion zone and the HAZ of Mn-B steel.
It recommended to avoid incomplete weld penetration when the examined steels are joined each other; in fact, the formation of notch in the fusion zone drastically reduces the mechanical properties of joints with the formation of fully brittle fractures.

REFERENCES

[1] M. Jeanneau, P. Pichant, La Rev. De Met., CIT, (2000) 1399.
[2] H. Hofmann, D. Mattissen, T.W. Schaumann, Materialwiss. Werkstofftech. 37 (2006) 716.
[3] T. Senuma, ISIJ Int., 41 (2001) 520.
[4] J. G. Speer, D. K. Matlock, JOM, 54 (2002) 19.
[5] E. K. Shakhpazov, A. I. Zaitsev, I. G. Rodionova, Metallurgist, 51 (2007) 262.
[6] H. Ding, C. Qiu, Z. Tang, J. Zeng, P. Yang, J. Iron and Steel Res., International, 18 (2011) 36.
[7] G. Frommeyer, U. Brüx, P. Neumann, ISIJ Int., 43 (2003) 438.
[8] O. Grässel, L. Krüger, G. Frommeyer, L. W. Meyer, Int. J. Plast., 16 (2000) 1391.
[9] L. Zhang, X. Liu, K. Shu, J. of Iron and Steel Res., 18 (2011) 45.
[10] K. Chung, K. Ahn, D. Yoo, K. Chung, M. Seo, S. Park, Int. J. Plast., 27 (2011) 52.
[11] G. Scavino, C. Di Salvo, P. Matteis, R. Sesana, D. Firrao, Met. Mat. Trans. A, 44 (2013) 787.
[12] P. Matteis, G. Scavino, F. D'Aiuto, D. Firrao, Steel Res. Int., 83 (2012), 950-956
[13] G. Scavino, F. D'Aiuto, P. Matteis, P. Russo Spena, D. Firrao, Met. Mat. Trans. A, 41 (2010) 1493.
[14] L. Mujica, S. Weber, W. Theisen. Scripta Mat., 66 (2012) 997.
[15] E. Koleva, Vacuum, 62 (2001) 151.
[16] K. Y. Benyounis, A. G. Olabi, M. S. J. Hashmi, J. Mat. Proc. Tech., 164-165 (2005) 978.
[17] O. Holovenko, M.G. Ienco, E. Pastore, M.R. Pinasco, P. Matteis, G. Scavino, D. Firrao, Met. It., 105 (2013) 3.
[18] K. Manonmani, N. Nurugan, G. Buvanasekaran, Int. J. Adv. Man. Tech., 44 (2007) 1125.
[19] R. Sharma, P. Molian, F. Peters, J. Man. Proc., 12 (2010) 73.
[20] L. Mujica, S. Weber, H. Pinto, C. Thomy, F. Vollertsen, Mat. Sci. Eng. A, 527 (2010) 2071.
[21] U. Reisgen, M. Schleser, O. Mokrov, E. Ahmed, Opt. Laser Tech., 44 (2012) 255.
[22] L. Mujica, S. Weber, C. Thomy, F. Vollertsen, Sci. Tech. Weld. Join., 14 (2009) 517.